Self-Similar Gold-Nanoparticle Antennas for a Cascaded Enhancement of the Optical Field

Christiane Höppener,[1,2] Zachary J. Lapin,[1] Palash Bharadwaj,[1] and Lukas Novotny[1,*]

[1]*Institute of Optics, University of Rochester, Rochester, New York 14627, USA*

[2]*Institute of Physics, University of Münster, 48149 Münster, Germany*

(Received 3 October 2011; revised manuscript received 3 May 2012; published 6 July 2012)

We experimentally demonstrate cascaded field enhancement by means of gold nanoparticle dimer and trimer antennas. The local field enhancement is probed by single-molecule fluorescence using fluorophores with high intrinsic quantum efficiency ($Q^0 > 80\%$). Using a self-similar trimer antenna consisting of 80, 40, and 20 nm gold nanoparticles, we demonstrate a fluorescence enhancement of 40 and a spatial confinement of 15 nm. Compared with a single gold nanoparticle, the self-similar trimer antenna improves the enhancement-confinement ratio by more than an order of magnitude. Self-similar antennas hold promise for high-resolution imaging and spectroscopy, ultrasensitive detection, and efficient single-photon sources.

DOI: 10.1103/PhysRevLett.109.017402 PACS numbers: 78.67.Bf, 68.37.Ef, 73.20.Mf, 78.68.+m

The unique optical properties of noble-metal nanoparticles are used in a wide range of applications, ranging from photovoltaics [1,2] and lasing [3,4] to biosensing [5] and cancer therapy [6]. These applications make use of the strongly enhanced local fields associated with the excitation of localized surface plasmon resonances. Noble-metal nanoparticles have also been studied as prototype optical antennas [7] for enhancing the photon emission from single-quantum emitters, such as single molecules, quantum dots, and ions [8–10]. These studies have shown that the enhancement of spontaneous emission (fluorescence) depends on both the excitation rate Γ_{exc} and the quantum yield Q of the quantum emitter.

For weak excitation fields (perturbation limit), the fluorescence rate Γ_{em} of a quantum emitter can be represented as

$$\Gamma_{\text{em}} = \Gamma_{\text{exc}} Q. \tag{1}$$

Accordingly, the fluorescence rate can be increased by enhancing either Γ_{exc} or Q. Since efficient emitters have an intrinsic quantum yield of $Q^0 \sim 1$, the emission rate can only be increased by enhancing the excitation rate Γ_{exc}. On the other hand, for poor emitters ($Q^0 \ll 1$) we can increase Γ_{em} by enhancing both Q and Γ_{exc}. Several studies have already demonstrated that the fluorescence enhancement depends strongly on the intrinsic quantum efficiency Q^0 [10–13]. High-Q^0 emitters yield low fluorescence enhancements whereas low-Q^0 emitters show strong fluorescence enhancements. For example, using a single 80 nm gold nanoparticle coupled to a quantum emitter one measures a fluorescence enhancement of 8–10 for high-Q^0 emitters [8,9] and >80 for low-Q^0 emitters such as yttrium ion metallofullerenes [10].

In general, the smaller the nanoparticle is, the lower the fluorescence enhancement will be. This can be understood by considering the nanoparticle's quasistatic polarizability $\alpha(\omega)$. The energy radiated by the emitter is related to the scattering cross section

$$\sigma_{\text{scatt}} = \frac{k^4}{6\pi\varepsilon_0^2}|\alpha(\omega)|^2, \tag{2}$$

where $k = \sqrt{\varepsilon_d}\omega/c$ is the wave vector of the surrounding medium. On the other hand, the energy dissipated by the nanoparticle is derived from the absorption cross section

$$\sigma_{\text{abs}} = \frac{k}{\varepsilon_0}\,\text{Im}[\alpha(\omega)]. \tag{3}$$

Because $\alpha \propto R^3$, R being the particle radius, the scattering cross section scales with R^6 whereas the absorption cross section depends on R^3. Therefore, absorption dominates over scattering for small particles. Thus, a strong fluorescence enhancement requires a large nanoparticle size, which on the other hand, provides poor localization [13–15]. Consequently, strong enhancement and high localization appear to be contradictory requirements. Here, we show that we can significantly boost the enhancement-localization ratio by using self-similar antennas consisting of coupled gold nanoparticles of decreasing size. For a trimer antenna consisting of 80, 40, and 20 nm nanoparticles, we achieve a fluorescence enhancement of ~40 and a localization of ~15 nm. Compared with a single gold nanoparticle, the trimer antenna improves the enhancement-localization ratio by more than an order of magnitude.

The cascaded field enhancement by a self-similar chain of nanoparticles was first proposed by Stockman and coworkers [16,17]. In this scheme, the radii of the particles in the chain scale as $R_{n+1} = \kappa R_n$ and the interparticle separations as $d_{n+1,n+2} = \kappa d_{n,n+1}$ with κ denoting a constant scaling factor and n the particle number. This geometry provides a multiplicative cascade effect: the largest particle enhances the incident field by a factor of f, the enhanced field then excites the next smaller particle which in turn enhances the field by another factor of f, and so on. This sequence leads to a concentration of light at the smallest

particle in the chain. Self-similar structures have been recently fabricated using both self-assembly techniques and top-down nanofabrication [18–20]. Kravets *et al.* have observed cascaded field enhancement in arrays of two and three gold nanodisks fabricated by electron beam lithography [20].

In this Letter, we experimentally demonstrate cascaded field enhancement with gold nanoparticles assembled into dimer and trimer antennas. Single molecules are used to probe the local field enhancement. The experimental configuration is illustrated in Fig. 1(a). A radially polarized laser beam ($\lambda = 633$ nm) is focused by means of a N.A. $= 1.4$ objective on the surface of a poly(methyl methacrylate) coated (2–5 nm) glass sample that supports randomly distributed Nile blue molecules ($Q^0 > 80\%$). A self-similar nanoparticle antenna consisting of a chain of gold nanoparticles of decreasing size is supported by a pointed quartz pipette and positioned into the center of the laser focus. The longitudinal field in the focus of the radially polarized beam excites the antenna, and the enhanced antenna field locally interacts with individual molecules on the sample surface. The antenna-sample separation can be controlled with Angstrom accuracy by means of a normal-force feedback loop. Fluorescence photons from single molecules are collected with the same objective and recorded with an avalanche photodiode while raster scanning the sample underneath the optical antenna or varying the antenna-sample distance. Dimer and trimer antennas are fabricated by sequential bottom-up assembly. Briefly, gold nanoparticles are dispersed on a clean glass substrate. An amino-silane functionalized quartz tip is first used to map out the distribution of the gold particles on the substrate and is then centered over a selected particle. Upon mechanical contact between gold particle and the functionalized tip, the particle attaches to the tip and can be lifted off the surface. With the use of 1,6-hexandithiol linker molecules, the attachment principle can be sequentially repeated to form dimers, trimers, tetramers, or higher multiparticle antennas. The finite size of the linker molecules assures that there is no electrical contact between individual particles (see Supplemental Material [21]). Figure 1(b) depicts a scanning electron micrograph of a typical self-similar trimer antenna fabricated following the procedure described above.

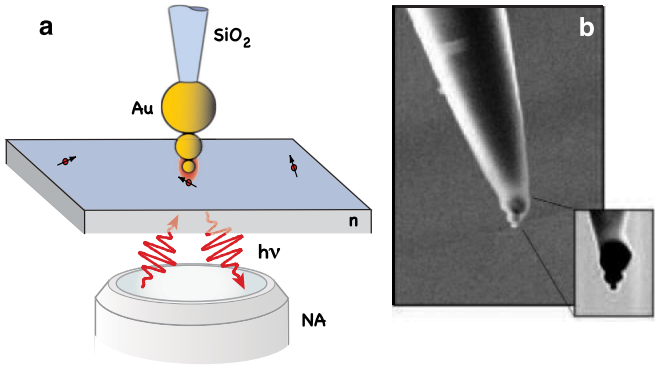

FIG. 1 (color online). (a) Illustration of the experimental configuration. A self-similar optical antenna made of discrete colloidal gold nanoparticles of decreasing size is placed next to a sample with randomly distributed Nile blue molecules. The antenna is irradiated by a tightly focused radially polarized laser beam with wavelength $\lambda_{exc} = 633$ nm. Fluorescence photons are recorded while the sample is raster scanned at a distance of ~5 nm underneath the antenna. (b) Scanning electron micrograph of a colloidal trimer antenna.

In a first step, we have compared a dimer antenna made of 80 and 40 nm gold nanoparticles with a single 40 nm gold nanoparticle antenna. The field localization of both antennas is defined by the 40 nm particle, but the local field is expected to be larger for the 80–40 nm dimer antenna because of cascaded field enhancement. Figure 2(a) shows a high-resolution fluorescence image of the single-molecule sample recorded with the 80–40 nm dimer antenna. Individual molecules can be clearly identified. The resolution is ~25 nm, and the fluorescence enhancement is ~20. The same sample has been reimaged with a single 40 nm nanoparticle antenna. In accordance with theoretical predictions, similar signal confinement is observed but the fluorescence enhancement is more than 4 times weaker (see Supplemental Material [21]). Figure 2(b) depicts the single-molecule emission spectrum in the presence (top curve) and absence of the 80–40 nm dimer antenna. A fluorescence enhancement of ~20 can be inferred from the two spectra. The shape of the spectrum remains largely unaffected by the presence of the dimer antenna (see Supplemental Material [21]). The dimer antenna yields a

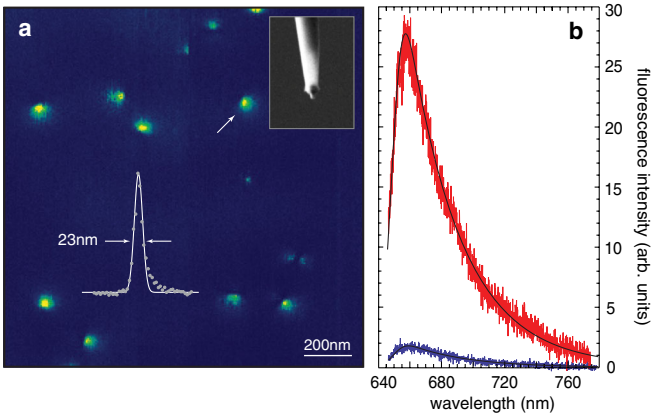

FIG. 2 (color online). Excitation of single-molecule fluorescence with a dimer antenna consisting of 80 and 40 nm gold nanoparticles. (a) Fluorescence image of the single-molecule sample. A line cut through the marked fluorescence spot indicates an optical confinement of 23 nm. The inset is a scanning electron micrograph of the dimer antenna. (b) Single-molecule emission spectrum with (upper curve) and without the dimer antenna (lower curve), revealing a fluorescence enhancement of ~20. Compared with a single 40 nm particle, the 80–40 nm dimer antenna provides a fourfold stronger fluorescence enhancement.

significantly higher fluorescence enhancement, underscoring the concept of cascaded field enhancement. While the large particle primarily interacts with the radiation field, the smaller particle provides the desired field localization.

Next, we add an additional 20 nm gold nanoparticle to the dimer. The resulting trimer antenna consists of a chain of 80, 40, and 20 nm nanoparticles. Note that the interparticle separation is kept constant at a distance of 2 nm by means of the dithiol linker molecules (see Supplemental Material [21]). The latter ensures that quantum size effects (e.g., screening and electron tunneling) are negligible [22]. Hence, charge transfer between individual spheres is inhibited for these structures. Theoretical studies have shown that the interaction between the nanoparticles leads to a redshift of the plasmon resonance [23]. In accordance, we find that the resonance of the 80–40–20 nm trimer antenna is redshifted from the plasmon resonance of an isolated spherical gold particle [cf. Fig. 3(b)]. The resonance is found to be at $\lambda = 590$ nm whereas the resonance of a single gold particle is at $\lambda = 530$ nm. Note that if the nanoparticles were in conductive contact the resulting plasmon resonance would shift into the near-infrared frequency regime (charge-transfer plasmon [24]). The separation of $\sim$2 nm ensures that the plasmon resonance remains in the visible part of the spectrum, which is a requirement for the single-molecule fluorescence experiments.

Figure 3(a) renders the calculated field distribution near the trimer antenna for an on-axis excitation with a focused radially polarized beam. The calculation is based on the multiple-multipole method [25]. The figure shows contours of constant $|\mathbf{E}|^2$ using a logarithmic scaling (factor of 2 between contour lines). The multiple-multipole calculation confirms the expected cascaded field enhancement; i.e., the field strength increases from the largest to the smallest particle. The intensity is highest in the gap between the two smaller particles, in agreement with the predictions by Li, Stockman, and Bergman [16], but the field is also significantly enhanced at the apex of the smallest particle. At the same time, the smallest particle provides sub-20 nm field localization. Similar calculations have been performed with a dipole source placed in front of the smallest particle and pointing along the particle chain. The resulting radiation pattern (data not shown) closely resembles that of a dipole source, suggesting incident radiation is mainly mediated by the largest particle in the chain.

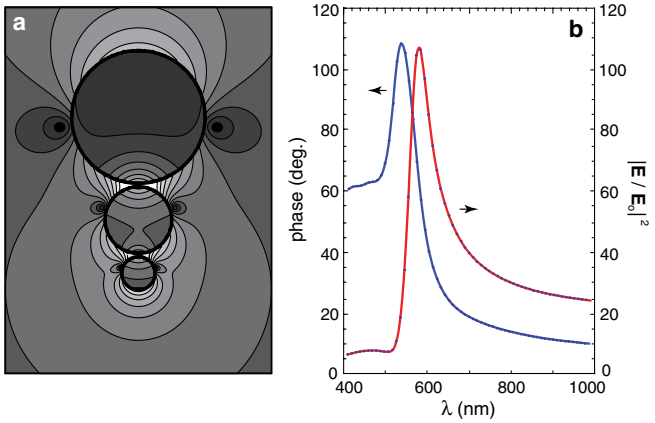

FIG. 3 (color online). (a) Field distribution near a self-similar trimer antenna consisting of gold nanoparticles with sizes 80, 40, and 20 nm. Contours of constant $|\mathbf{E}|^2$. Logarithmic scaling with factor of two between contour lines. (b) Spectrum at the apex of the trimer antenna. The curves show the phase relative to the incident field and the intensity enhancement.

Following the outlined theoretical considerations, we have performed single-molecule fluorescence experiments using 80–40–20 nm gold nanoparticle trimer antennas, similar to the one shown in Fig. 1(b). A fluorescence map of the single-molecule sample is shown in Fig. 4(a). Line cuts through individual fluorescence spots yield a resolution of 15 nm, as seen in the inset. This resolution is expected on the basis of the smallest particle size. In general, we observe that the resolution (signal confinement) is slightly better than the true particle size. An 80 nm particle yields a resolution of $\sim$60 nm, a 40 nm particle yields a resolution of 25 nm, and a 20 nm particle yields a resolution of 15 nm. Resolution is better than the particle size because of the curvature of the particle surface and the particular field distribution. Finally, to demonstrate the strong localization of fields along the z direction at the apex of the trimer, we recorded a fluorescence approach curve as shown in Fig. 4(b). The sharp increase in signal over the last 15 nm conclusively proves that the localization arises due to the foremost 20 nm diameter particle.

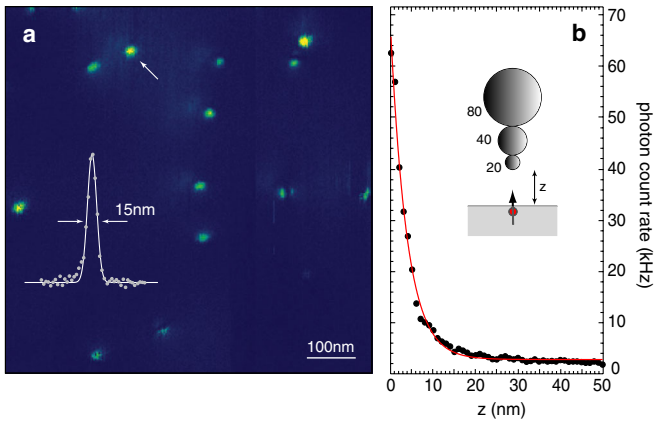

FIG. 4 (color online). Excitation of single-molecule fluorescence with a trimer antenna consisting of 80, 40, and 20 nm gold nanoparticles. (a) Fluorescence image of the single-molecule sample. Inset: Line cut through the single fluorescence spot marked by the arrow. (b) Fluorescence from a single z-oriented molecule recorded as a function of distance from a trimer antenna. The steep rise of fluorescence counts for separations smaller than 15 nm is due to strong field localization along the z axis at the apex of the trimer antenna.

The maximum fluorescence enhancement for the trimer antenna is ~40, an improvement over the dimer antenna. Note, however, that the measured fluorescence not only depends on the local field enhancement but also on the quantum yield [cf. Eq. (1)]. Because the nonradiative decay rate is higher for molecules near small nanoparticles [14], fluorescence quenching is more severe for the trimer antenna than for the dimer antenna. Thus, single-molecule fluorescence measurements provide a very conservative estimate of the local field enhancement. Compared to a single 80 nm nanoparticle, the trimer antenna improves the enhancement-localization ratio by a factor of 15, and compared to a 20 nm nanoparticle, the improvement is almost a factor of 30. Finally, it should be noted that the highest enhancements are seen for vertically oriented molecules, whereas in-plane oriented molecules yield a factor ~3 lower fluorescence enhancement.

In conclusion, we have experimentally demonstrated cascaded field enhancement using self-similar antennas made of colloidal gold nanoparticles. For an 80–40–20 nm trimer antenna we obtain a localization of 15 nm and a fluorescence enhancement of 40 for molecules with high intrinsic quantum yield efficiency ($Q^0 \sim 0.8$). We have shown that the largest particle is responsible for the interaction with the radiation field while the smallest particle is responsible for field localization. The high enhancement-localization ratio achieved with the self-similar antenna geometry improves the resolution in fluorescence imaging and provides high detection sensitivity. Self-similar antennas also hold promise for high-efficiency single-photon sources and ultralow-noise photodetectors.

This research was funded by the U.S. Department of Energy (Grant No. DE-FG02-01ER15204). C. H. thanks the Ministerium für Innovation, Wissenschaft und Forschung des Landes Nordrhein-Westfalen, Germany, for additional support.

*http://www.nano-optics.org

[1] H. A. Atwater and A. Polman, Nature Mater. **9**, 205 (2010).
[2] K. Nakayama, K. Tanabe, and H. A. Atwater, Appl. Phys. Lett. **93**, 121904 (2008).
[3] M. I. Stockman, New J. Phys. **10**, 025031 (2008).
[4] M. A. Noginov, G. Zhu, A. M. Belgrave, R. Bakker, V. M. Shalaev, E. E. Narimanov, S. Stout, E. Herz, T. Suteewong, and U. Wiesner, Nature (London) **460**, 1110 (2009).
[5] J. N. Anker, W. P. Hall, O. Lyandres, N. C. Shah, J. Zhao, and R. P. van Duyne, Nature Mater. **7**, 442 (2008).
[6] C. Loo, A. Lin, L. Hirsch, M. H. Lee, J. Barton, N. Halas, J. West, and R. Drezek, Technol. Cancer Res. Treat. **3**, 33 (2004).
[7] P. Bharadwaj, B. Deutsch, and L. Novotny, Adv. Opt. Photon. **1**, 438 (2009).
[8] S. Kühn, U. Hakanson, L. Rogobete, and V. Sandoghdar, Phys. Rev. Lett. **97**, 017402 (2006).
[9] P. Bharadwaj and L. Novotny, Nano Lett. **11**, 2137 (2011).
[10] P. Bharadwaj and L. Novotny, J. Phys. Chem. C **114**, 7444 (2010).
[11] A. Wokaun, H.-P. Lutz, A. P. King, U. P. Wild, and R. R. Ernst, J. Chem. Phys. **79**, 509 (1983).
[12] R. Bardhan, N. K. Grady, J. R. Cole, A. Joshi, and N. J. Halas, ACS Nano **3**, 744 (2009).
[13] H. Eghidi, K. G. Lee, X.-W. Chen, S. Götzinger, and V. Sandoghdar, Nano Lett. **9**, 4007 (2009).
[14] P. Anger, P. Bharadwaj, and L. Novotny, Phys. Rev. Lett. **96**, 113002 (2006).
[15] C. Höppener, R. Beams, and L. Novotny, Nano Lett. **9**, 903 (2009).
[16] K. Li, M. I. Stockman, and D. J. Bergman, Phys. Rev. Lett. **91**, 227402 (2003).
[17] M. I. Stockman, V. M. Shalaev, M. Moskovits, R. Botet, and T. F. George, Phys. Rev. B **46**, 2821 (1992).
[18] B. Ding, Z. Deng, H. Yan, S. Cabrini, R. N. Zuckermann, and J. Bokor, J. Am. Chem. Soc. **132**, 3248 (2010).
[19] S. Bidault, F. J. G. de Abajo, and A. Polman, J. Am. Chem. Soc. **130**, 2750 (2008).
[20] V. G. Kravets, G. Zoriniants, C. P. Burrows, F. Schedin, C. Casiraghi, P. Klar, A. K. Geim, W. L. Barnes, and A. N. Grigorenko, Phys. Rev. Lett. **105**, 246806 (2010).
[21] See Supplemental Material at http://link.aps.org/supplemental/10.1103/PhysRevLett.109.017402 for transmission electron micrographs of the dimer antennas, fluorescence emission spectra using the trimer antenna, and additional fluorescence images.
[22] P. Song, P. Nordlander, and S. W. Gao, J. Chem. Phys. **134**, 074701 (2011).
[23] R. Kappeler, D. Erni, C. Xudong, and L. Novotny, J. Comput. Theor. Nanosci. **4**, 686 (2007).
[24] O. Perez-Gonzalez, N. Zabala, A. G. Borisov, N. J. Halas, P. Nordlander, and J. Aizpurua, Nano Lett. **10**, 3090 (2010).
[25] L. Novotny and B. Hecht, *Principles of Nano-Optics* (Cambridge University Press, Cambridge, England, 2006).